anticipated that approach of the peracid would occur from the less hindered α face of **7**; the resultant highly strained intermediate epoxide would then suffer in situ acid-catalyzed trans diaxial ring opening to yield **8a**. That our structural assignment for this compound was correct was confirmed by a single-crystal X-ray analysis of the derived benzoate ester (**8b**).[10,13] Final conversion of **8a** to **4a**[10] proceeded in 60% overall yield via protection of the hydroxyl group as the TES derivative (Et_3SiCl, Et_3N, DMAP, CH_2Cl_2, 25 °C) and execution of the Reich–Sharpless[14] phenyl selenation–oxidative elimination sequence.

With **4a** in hand, our plan for elaboration of dechloromycorrhizin A (**1c**) called for the addition of *trans*-bis(1-propenyl)copper lithium,[15] followed by desilylation (Bu_4NF), oxidation (Swern oxidation,[21] followed by SeO_2/pyridine/*t*-BuOH), and hydrolysis (aq HBF_4/dioxane) of the mixed methyl ketal of **1c**. It was anticipated (hoped) that the chlorine at C(3) could then be introduced via a chlorination–dehydrochlorination sequence to afford mycorrhizin A (**1a**). We were, in fact, successful in preparing dechloromycorrhizin A (**1c**) via this strategy in 12.6% overall yield from **4a**. Unfortunately, introduction of chlorine at C(3) proved problematic. We were, however, encouraged by the observations of Miller and McGarvey,[16] who demonstrated that vinylsilanes could be cleanly converted to vinyl chlorides of inverted configuration via a halogenation–desilylation protocol.

Toward this end addition of **4a** to a solution of the cuprate derived from (*E*)-(1-lithio-1-propenyl)trimethylsilane[17] resulted in the formation of **9a**[10] in 75% yield after selective O-desilylation (1.5 equiv of Bu_4NF/THF/0 °C). Also present, in 10% yield, was the corresponding *Z* isomer (**9b**), which could be separated chromatographically from **9a**.[19]

Swern oxidation[21] of **9a** [$(COCl)_2/Me_2SO/Et_3N$] gave the corresponding dione[10a] (mp 98–100 °C) in 65% yield. Further oxidation with SeO_2 (*t*-BuOH/pyridine, at reflux, 5 h) then afforded a 2:1 mixture of **10a**[10a] and **10b**,[10] respectively, in a combined yield of 55%. As anticipated, treatment of **10b** with chlorine at −75 °C, followed by brief exposure to KF in Me_2SO[16] at 25 °C gave racemic mycorrhizin A in 73% yield identical in all respects (IR, 250-MHz NMR, and TLC) with an authentic sample kindly provided by Wickberg and Trofast. Alternatively, exposure of **10a** to the same conditions produced the mixed methyl ketal of mycorrhizin A in 60% yield. The latter was then hydrolyzed [50% HBF_4/dioxane (1:6)/80 °C, 15 min, 60%] to mycorrhizin A via the Wickberg–Trofast protocol.[22]

In summation, the first total synthesis of (±)-mycorrhizin A and dechloromycorrhizin A has been achieved. Studies to improve this sequence, including a chiral synthesis of mycorrhizin A (**1a**), and to effect the total synthesis of gilmicolin by exploiting the α-hydroxyl functionality at C(12) to introduce oxygen at C(2) in a stereocontrolled fashion will be reported in due course.

Acknowledgment. It is a pleasure to acknowledge the support of this investigation by the National Institutes of Health (Institute of General Medical Sciences) through Grant No. GM-24680. In addition, we thank S. T. Bella of the Rockefeller University for the microanalyses and Drs. G. Furst and T. Terwilliger of the University of Pennsylvania for aid in recording and interpretation of the high-field NMR and mass spectra.

(13) Unpublished results of P. Carroll and J. Safaryn of our laboratory.
(14) H. J. Reich, I. C. Reich, and J. M. Renga, *J. Am. Chem. Soc.*, **95**, 5813 (1973); K. B. Sharpless and R. F. Lauer, *ibid.*, 2697.
(15) G. Linstrumelle, J. K. Krieger, and G. M. Whitesides, *Org. Synth.*, **55**, 103 (1976).
(16) R. B. Miller and G. McGarvey, *J. Org. Chem.*, **43**, 4424 (1978).
(17) Prepared from (*Z*)-(1-bromo-1-propenyl)trimethylsilane[18] by halogen–metal exchange with *tert*-butyllithium.
(18) D. Seyferth, J. Lefferts, and R. L. Lambert, Jr., *J. Organomet. Chem.*, **142**, 39 (1977).
(19) The small amount of **9b** formed in the cuprate addition is due to the configurational instability of (1-lithio-1-alkenyl)trimethylsilanes at temperatures above −70 °C.[20]
(20) G. Zweifel, R. E. Murray, and H. P. On, *J. Org. Chem.*, **46**, 1292 (1981).
(21) A. J. Mancuso, S.-L. Huang, and D. Swern, *J. Org. Chem.*, **43**, 2480 (1978).
(22) Hydrolysis of the mixed methyl ketal of mycrorrhizin had been carried out by Trofast and Wickberg during their isolation studies; see ref 2 and 7.

A Dinuclear Rhodium Complex with an Octahedral Rhodium(III) and a Square-Planar Rhodium(I) Center

Eric B. Meier, R. R. Burch, and E. L. Muetterties*

Department of Chemistry, University of California Berkeley, California 92720

V. W. Day*

Department of Chemistry, University of Nebraska Lincoln, Nebraska 68588 and The Crystalytics Company, Lincoln, Nebraska 68501

Received December 28, 1981

A family of polynuclear rhodium hydrides of the form $\{HRh(PY_3)_2\}_n$[1] has been prepared, and we describe here the chemistry of $(\mu\text{-H})_2Rh_2\{P[N(CH_3)_2]_3\}_4$. Seminal are the structural features of an intermediate in the olefin hydrogenation cycle catalyzed by the dimer. This intermediate is distinguished by an octahedral rhodium(III) center and a square-planar rhodium(I) center joined through a common edge defined by the two bridging hydride ligands. This unique structure is the paradigm for the intermediate preceding olefin complexation in olefin hydrogenation cycles catalyzed by these polynuclear rhodium hydrides.

The dimer, $(\mu\text{-H})_2Rh_2\{P[N(CH_3)_2]_3\}_4$, has in the solution state a near coplanar set of framework atoms, $P_2RhH_2RhP_2$, as judged by the NMR data[2] and is isostructural with $(\mu\text{-H})_2Rh_2[P(O\text{-}i\text{-}C_3H_7)_3]_4$. Both these dimers are active catalyst precursors for olefin hydrogenation. In this catalytic cycle, the first step is hydrogen addition,[1a] which is reversible for both dimers (see eq 1). However, the reverse step, hydrogen elimination, is slower

$$H_4Rh_2(PY_3)_4 \rightleftharpoons (\mu\text{-H})_2Rh_2(PY_3)_4 + H_2 \qquad (1)$$

for the phosphine derivative, a feature that facilitated isolation of the tetrahydride in single-crystal form (from toluene at −40 °C).[3]

Single crystals of $H_4Rh_2\{P[N(CH_3)_2]_3\}_4 \cdot 0.5CH_3C_6H_5$ (**1**) were triclinic, space group $P\bar{1}$-C_i^1 (No. 2), with a = 10.851 (3) Å, b = 13.326 (4) Å, c = 17.098 (5) Å, α = 85.93 (2)°, β = 95.02 (2)°, γ = 114.87 (2)°, and Z = 2 (ρ_{calcd} = 1.689 g cm^{-3}; μ_a (Mo K$\bar{\alpha}$) = 0.89 mm^{-1}). Three-dimensional X-ray diffraction data were collected (20 ± 1 °C) for 15 304 independent reflections

(1) Sivak, A. J.; Muetterties, E. L. *J. Am. Chem. Soc.* **1979**, *101*, 4878. (b) Burch, R. R.; Muetterties, E. L.; Day, V. W. *Organometallics* **1982**, *1*, 188.
(2) ^{1}H NMR (toluene-d_8, +28 °C, 180 MHz) δ + 2.2 (m, NCH_3), −9.2 (q of t, $J_{Rh\text{-}H}$ = 33.3 Hz, $J_{P\text{-}H}$ = 30.7 Hz); $^1H\{^{31}P\}$ NMR (toluene-d_8, +20 °C, 180 MHz) δ +2.2 (m, NCH_3), −9.2 (t, $J_{Rh\text{-}H}$ = 33.3 Hz); $^1H\{^{31}P\}$ NMR (toluene-d_8, −70 °C, 180 MHz) δ +2.2 (m, NCH_3), −9.2 (t, $J_{Rh\text{-}H}$ = 33.3 Hz); $^{31}P\{^1H\}$ NMR (toluene-d_8, +20 °C, 72.9 MHz) δ +132.2 (relative to 85% H_3PO_4) AA′A″A‴XX′ pattern characteristic of $(HRhP_2)_2$ compounds, but poorly resolved presumably due to the nitrogen quadrupolar nuclei; $^{31}P\{^1H\}$ NMR (toluene-d_8, −50 °C, 72.9 MHz) δ +132.5 (br d) (relative to 85% H_3PO_4).
(3) ^{1}H NMR (toluene-d_8, 20 °C, 250 MHz) δ +2.79 (t, J = 5.2 Hz, NCH_3), +2.62 (d, J = 8.8 Hz, NCH_3), −10.5 (m, H_b), −16.8 (approximate quin. of m, H_t, $J \simeq$ 18 Hz). When the sample was cooled to −70 °C, the chemical shifts were temperature independent but there was substantial line broadening. $^1H\{^{31}P\}$ NMR (toluene-d_8, 20 °C, 180 MHz) δ +2.79, +2.62 −10.5 (t, $J_{Rh\text{-}H}$ = 52.5 Hz), −16.8 (d, $J_{Rh\text{-}H}$ = 17.5 Hz); $^1H\{^{31}P\}$ NMR (toluene-d_8, −70 °C, 180 MHz) δ +2.79, +2.62, −10.5 (t of m, $J_{Rh\text{-}H}$ = 26.6 Hz), −16.8 (br s); $^{31}P\{^1H\}$ NMR (toluene-d_8, 72.9 MHz) δ +147.3 (d, $J_{Rh\text{-}P}$ = 142.5 Hz), +146.5 (d of d, $J_{Rh\text{-}P}$ = 217 Hz, $J_{Rh\text{-}P}$ = 3.3 Hz) (relative to 85% H_3PO_4); $^{31}P\{^1H\}$ NMR (toluene-d_8, −77 °C, 72.9 MHz) δ +147.8 (d, $J_{Rh\text{-}P}$ = 142.5 Hz), +148.3 (d, $J_{Rh\text{-}P}$ = 217 Hz) (relative to 85% H_3PO_4) (the temperature dependence of the $^{31}P\{^1H\}$ NMR spectra we attribute to excited-state contributions); ν(Rh–H) = 1995 cm^{-1} (pentane).

0002-7863/82/1504-2661$01.25/0

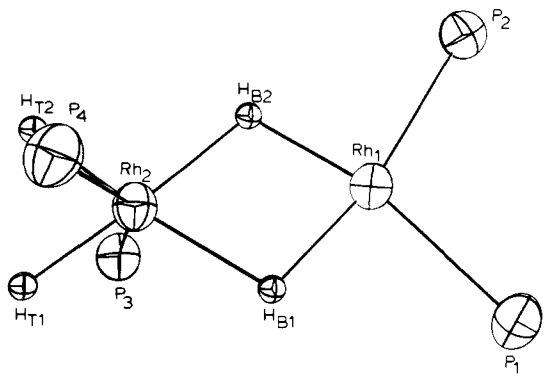

Figure 1. Perspective ORTEP drawing of the immediate metal coordination spheres in $H_4Rh_2\{P[N(CH_3)_2]_3\}_4$ (**1**). Average values of bond lengths and angles for chemically distinct groups of atoms are as follows: Rh_1–Rh_2, 2.734 (1) Å; Rh_1–P, 2.231 (1) Å; Rh_2–P, 2.288 (1) Å; Rh_1–H_B, 1.68 (3) Å; Rh_2–H_B, 1.77 (3) Å; Rh_2–H_T, 1.52 (3) Å; Rh_1–H_B, 1.68 (3) Å; Rh_2–H_B, 1.77 (3) Å; Rh_2–H_T, 1.52 (3) Å; P–Rh_1–P, 103.4 (1)°; H_{B1}–Rh_1–H_{B2}, 77 (1)°; P–Rh_1–H, cis, 90 (1)°, trans, 167 (1)°; P–Rh_2–P, 154.8 (1)°; H_{T1}–Rh_2–H_{T2}, 74 (2)°.

having $2\theta_{Mo\,K\bar{\alpha}} < 63.7°$ (the equivalent of 1.5 limiting Cu K$\bar{\alpha}$ spheres) on a Nicolet $P\bar{1}$ autodiffractometer using graphite-monochromated Mo K$\bar{\alpha}$ radiation and full (1°-wide) ω scans. The two rhodium atoms were located by using "direct methods" techniques and the remaining nonhydrogen and hydrogen atoms with difference Fourier techniques. Structural parameters of all 121 independent (45 anisotropic nonhydrogens[4a] and 76 isotropic hydrogen) atoms were refined to convergence [R (unweighted, based on F) = 0.032 for 11 100 independent reflections having $I > 3\sigma(I)$] by using cascade-blocked least-squares techniques.[4b]

The structural analysis revealed that the crystal is composed of ordered $H_4Rh_2\{P[N(CH_3)_2]_3\}_4$ (**1**) molecules as illustrated in Figure 1 and disordered toluene molecules of crystallization. One metal atom (Rh_1) in **1** is formally a d^8 Rh(I) center and the other (Rh_2) a d^6 Rh(III) center. The Rh(I) atom has a square-planar coordination geometry through direct bonding to two cis-phosphine phosphorus atoms and two bridging hydride hydrogen atoms. The coordination geometry for the Rh(III) atom is octahedral, although the intraligand angles depart from the idealized regular octahedral angles in an explicable fashion, with two phosphine phosphorus atoms occupying trans sites, two terminal hydride hydrogen atoms one set of cis coordination sites, and two bridging hydride hydrogen atoms the remaining set of cis sites. An appropriate molecular orbital description of **1** has the two bridging hydride ligands and the two metal atoms forming two four-center, two-electron bonds to generate, in a formal context, 16- and 18-electron valence-shell configurations for Rh_1 and Rh_2, respectively. Thus, there is a potentially reactive site in the ground-state configuration of **1**, a feature consistent with the chemistry discussed below.

Although **1** is not required to possess any rigorous crystallographic symmetry, the edge-shared coordination polyhedron approximates rather closely idealized C_{2v} symmetry with the pseudo C_2 axis passing through both metal atoms. The first idealized mirror plane contains both metal atoms, all four hydride hydrogen atoms, and the two phosphorus atoms bonded to Rh_1 (these eight atoms are coplanar to within 0.07 Å); the second idealized mirror plane contains both Rh atoms and both phosphorus atoms bonded to Rh_2 (these four atoms are coplanar to within 0.03 Å, and their least-squares mean plane makes a dihedral angle of 90.0° with that of the eight-atom grouping for the first idealized mirror plane). The metal–ligand atom distances are uniformly shorter as expected for the four-coordinate Rh(I) atom than for the six-coordinate Rh(III) atom. Electronic[5] and steric considerations would project interligand bond angles of <90° for cis H_B–M–H_B and H_T–M–H_T and >90 or <180° for cis or trans P–M–P, parametric features that are extant in this complex. In **1**, the Rh–H and Rh–P distances of 1.68 and 2.23 Å for square-planar Rh_1 compare well, within experimental error, respectively, with those of the planar dimer, $(\mu\text{-}H)_2Rh_2[P(O\text{-}i\text{-}C_3H_7)_3]_4$, of 1.81 and 2.17 Å, respectively.[6]

In solution, $H_4Rh_2\{P[N(CH_3)_2]_3\}_4$ exhibited ^1H and $^{31}P\{^1H\}$ NMR spectra[3] fully consistent with the solid-state structure. This phase-persistent structural feature is qualitatively different from the structural behavior of the hydrogen adduct derived from $(\mu\text{-}H)_2Rh_2[P(O\text{-}i\text{-}C_3H_7)_3]_4$. No crystallographic data are available yet for this phosphite-based tetrahydride, but the NMR data[1a] definitively establish that in solution the ground-state structure has *three* bridging hydride ligands of two environmental classes and one terminal hydride ligand. On the basis of an interpretation[1a] of the temperature dependence of the ^1H NMR spectra, an excited-state dimeric structure, **3**, with Rh(I) and Rh(III)

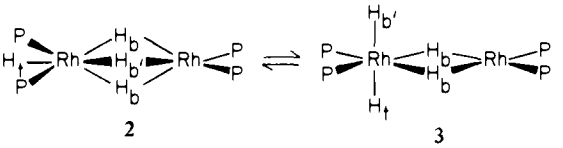

2 **3**

centers was postulated[1a] as shown in eq 2 with the postulated ground-state form **2**. The excited state, **3** further postulated[1a] to be the active intermediate in olefin hydrogenation, differs from the structure of **1** only in a transposition of terminal H and P ligating atoms for Rh(III). This excited-state species should be stereochemically identical with **1**—hence, on the basis of the trans H–P relationships[1a] preserved in the dynamic NMR process and observed for $H_4Rh_2[P(O\text{-}i\text{-}C_3H_7)_3]_4$ and on the stereochemistry established for **1**, the ground- and excited-state (solution phase) representations for $H_4Rh_2[P(O\text{-}i\text{-}C_3H_7)_3]_4$ perhaps are better represented as shown in eq 3 as **4** and **5**, respectively.

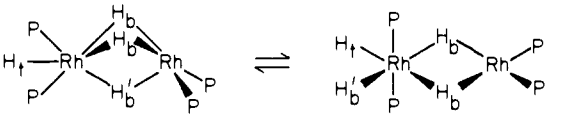

4 **5**

$H_4Rh_2\{P[N(CH_3)_2]_3\}_4$ is an intermediate in the olefin hydrogenation reaction catalyzed by the dimer; it reacted instantaneously at 20 °C with olefin to produce alkane and $(\mu\text{-}H)_2Rh_2\{P[N(CH_3)_2]_3\}_4$. Both $(\mu\text{-}H)_2Rh_2\{P[N(CH_3)_2]_3\}_4$ and $(\mu\text{-}H)_2Rh_2[P(O\text{-}i\text{-}C_3H_7)_3]_4$ catalyzed the hydrogenation of olefins at comparable rates, and the *dominant* first reaction step in the catalytic cycle was hydrogen addition, and the end products were alkane and the rhodium dimers. However, the phosphine dimer chemistry does differ qualitatively from that of the phosphite dimer: whereas $(\mu\text{-}H)_2Rh_2[P(O\text{-}i\text{-}C_3H_7)_3]_4$ did not react with ethylene at 20 °C, $(\mu\text{-}H)_2Rh_2\{P[N(CH_3)_2]_3\}_4$ did to form two new intermediate dimeric hydrides. This latter reaction was fast but still is much slower than hydrogen addition to the dimer. The key point here is the structural and chemical differentiation rendered in the chemistry of $H_2Rh_2(PY_3)_4$ species by the relatively subtle substitution of a phosphite by an aminophosphine.[7] Our family of $\{HRh(PY_3)_2\}_x$ species presents a unique opportunity to assess structure, stereochemistry, chemistry, and catalysis in coordinately *unsaturated* clusters.

Acknowledgment. We acknowledge support by the National Science Foundation, the loan of rhodium chloride by Johnson

(4) (a) 42 nonhydrogen atoms from the dimer and 3 from the disordered toluene, on average. (b) All calculations were performed on a Data General Eclipse S-200 computer by using locally modified versions of the Nicolet EXTL or SHELXTL interactive software systems.

(5) (a) Hoffmann, R.; Howell, J. M.; Rossi, A. R. *J. Am. Chem. Soc.* **1976**, *98*, 2484. (b) Elian, M.; Hoffmann, R. *Inorg. Chem.* **1975**, *14*, 1058.

(6) Teller, R. G.; Williams, J. M.; Koetzle, T. F.; Burch, R. R.; Gavin, R. M.; Muetterties, E. L. *Inorg. Chem.* **1981**, *20*, 1806.

(7) Generally, the $\{HRh(PY_3)_2\}_x$ species are resistant to fragmentation[1a,8] to mononuclear complexes. It is notable that solution-state mixtures of $H_2Rh_2\{P[N(CH_3)_2]_3\}_4$ and $H_2Rh_2[P(O\text{-}i\text{-}C_3H_7)_3]_4$ in the presence and absence of H_2 gave no evidence of formation of $\{[(CH_3)_2N]_3P\}_2Rh(\mu\text{-}H)_2Rh[P(O\text{-}i\text{-}C_3H_7)_3]_2$.

(8) Burch, R. R.; Muetterties, E. L.; Schultz, A. J.; Gebert, E. G.; Williams, J. M. *J. Am. Chem. Soc.* **1981**, *103*, 5517.

Matthey, Inc., the Miller Institute for Research in Basic Science for a grant in the form of a Miller Professorship to E.L.M., the National Science Foundation for a graduate fellowship for R.R.B. (1979–1982), and the Swiss National Science Foundation for a postdoctoral fellowship for E.B.M.

Registry No. 1, 81277-27-2; $(\mu\text{-H})_2Rh_2\{P[N(CH_3)_2]_3\}$, 81277-05-6; $\{ClRh(C_2H_4)_2\}_2$, 12081-16-2; tris(dimethylamino)phosphine, 1608-26-0.

Supplementary Material Available: Preparation of the $(HRhP_2)_2$ dimer and characterization of **1**, three tables listing atomic coordinates, selected bond distances and angles, and thermal parameters for nonhydrogen atoms in crystalline $H_4Rh_2\{P[N(CH_3)_2]_3\}_4$, and Figure 2, a full-perspective ORTEP drawing of the tetrahydride **1** (11 pages). Ordering information is given on any current masthead page.

Temperature-Regulated Release of Alkali Metal Salts from Novel Polymeric Crown Ether Complexes[1]

Abraham Warshawsky* and Nava Kahana[2]

Department of Organic Chemistry
The Weizmann Institute of Science, Rehovot, Israel
Received December 28, 1981

Early studies[3] on the thermodynamics of cation–macrocyclic crown ether interaction have shown that $\Delta H°$ and $\Delta S°$ values for complexation are usually negative and small.[4] Consequently the sign and value of the free energy, $\Delta G°$, may depend on the absolute temperatures, since $\Delta G° = \Delta H° - T\Delta S°$. In homogeneous systems this has little significance. However, in a heterogeneous system, such as equilibria between insoluble polymer and solution, it is reasonable to assume that the opposing effects of $\Delta H°$ and $\Delta S°$ could be exploited to induce temperature-regulated release of salts from their insoluble polymeric crown ether complexes, as follows:

$$[P]\text{-}(CE) + MX \underset{T_2}{\overset{T_1}{\rightleftharpoons}} [P]\text{-}(CE)MX \qquad T_2 > T_1$$

[P] = polymer, CE = crown ether, M = alkali metal, X = halide

Polymeric materials carrying pendant crown ether groups have been prepared by: (i) direct polymerization of vinylbenzo crown ethers;[5] (ii) condensation polymerization of dibenzo crown ethers with formaldehyde.[6]

Recently, we presented a different approach, based on a one-step in situ cyclization reaction.[7] Thus, a nucleophilic substitution reaction between two electrophilic centers (benzyl halide groups, part of the polymeric matrix) and a cation-templated polyglycol takes place, leading to large macrocycles. The so-called "pseudo crown ether" anchored to a macroporous matrix structure showed high affinity for transition-metal complex anions (in their conjugate acid form), with excellent reversibility in complexation–decomplexation.

Now this approach has been extended to the synthesis of polymeric crown ethers carrying pendant macrocyclic rings. This was accomplished by reversing the role of the functional groups and putting the nucleophilic centers on the polymeric matrix.

Scheme I

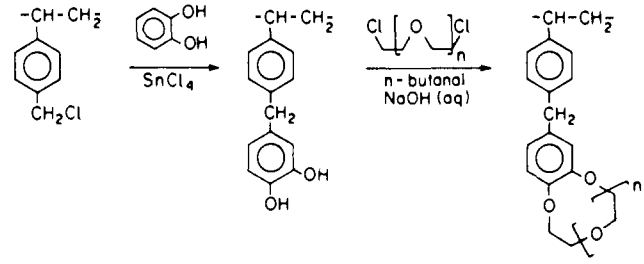

Table I. Synthesis of Polymeric Crown Ethers by Condensation of Polymer-Bound Catechol and Polyglycol Dihalides

			molecular fraction of unit		
polymer	no.	glycol dihalide	$-C_6H_4CH_2Cl$	$-C_6H_3(OH)_2$	$-C_6H_3$ crown
crown-4	NK-37	triethylene	0.08	0.22	0.65
crown-5	NK-40	tetraethylene	0.04	0.21	0.64
crown-6	NK-41	pentaethylene	0.02	0.21	0.60
crown-8	NK-43	heptaethylene	0.00	0.27	0.86

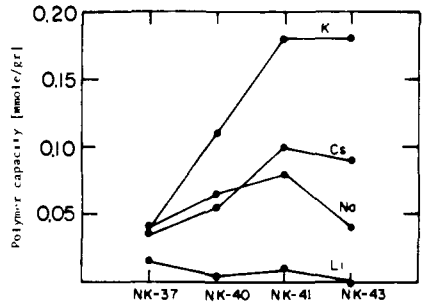

Figure 1. Ion recognition patterns for polymeric crown ethers (see Table I) expressed as polymer capacity from 0.01 M solutions in CH_3OH at 20 °C.

Thus, the alkylation of catechol with (chloromethyl)styrene–divinylbenzene copolymer (see Scheme I), produces the polymer-bound catechol, which upon reaction with a series of polyglycol dihalides affords macrocyclic polymeric benzo crown ethers in fair yields.

The degree of conversion of the catechol groups into macrocyclic ether groups and the residual concentration of diol groups were estimated from elemental analysis, weight-gain data, and the analysis of dinitrophenyl derivatives of the residual diol groups. The description and properties of the polymeric crown ethers are presented in Table I.

Next, the ion-coordination patterns for the polymeric crowns were determined by using distribution and column techniques. Equilibrium distribution values in methanol in the temperature range 20–60 °C, for the perchlorate, thiocyanate, or bromide salts, have led to the following conclusions: (1) The spheric recognition patterns, typical of crown ethers in solution, are fully reproduced in the polymeric analogues. Figure 1 shows the relative ion capacities for polymeric benzo crown-4, crown-5, crown-6, and crown-8. Accordingly, the order of binding constants is K > Cs > Na > Li for polymeric benzo crown-6 and benzo crown-8 and K > Cs ≃ Na > Li for polymeric benzo crown-4 and benzo crown-5. (2) The highest binding constants are for polymeric benzo crown-6, as anticipated from data for the corresponding benzo crown-6.[3] (3) The polymers bind alkali metal cations by two mechanisms: the residual catechol groups by an ion-exchange mechanism, and the crown groups by a salt-coordination mechanism; the second mechanism is temperature dependent. Consequently, a column packed with polymeric benzo crown-6 can be saturated with KCl, and as Figure 2 shows, a sudden thermal increase of 40 °C causes a spontaneous elution, by "thermal shock", and a 3-fold increase in the eluant of the original ion concentration. Quantitative release of all the bound salt is observed.

(1) Presented at the Second Chemical Congress of the North American Conference, San Francisco, CA, August 24–29, 1980.
(2) Taken in part from the M.Sc. Thesis of Nava Kahana, the Feinberg Graduate School, The Weizmann Institute of Science, 1980.
(3) Izatt, R. M.; Eatough, D. J.; Christensen, J. J. "Structure and Bonding"; Springer-Verlag: Berlin, West Germany, 1973; Vol. 16, pp 161–189 and references therein.
(4) The following $-\Delta H°$ (in kcal/mol) and $-\Delta S°$ (in Cal/(Kmol)) were reported in ref 3, Table 2: K^+ (3.88, 3.8), Rb^+ (3.33, 4.2), Cs^+ (2.41, 3.7); L = dicyclohexano-18-crown-6.
(5) Smid, J. et al. *Pure Appl. Chem.* **1979**, *51*, 111.
(6) Blasiuss, E. et al. *Fresenius' Z. Anal. Chem.* **1977**, *284*, 337 and references therein.
(7) Warshawsky, A. Kalir, R.; Deshe, A.; Berkovitz, H.; Patchornik, A. *J. Am. Chem. Soc.* **1979**, *101*, 4249.

0002-7863/82/1504-2663$01.25/0